Application of Nuclear Magnetic Resonance Imaging in Blood Flow Estimation

E. O. Odoh and D. K. De*
Department of Physics, Federal University of Technology,
P.M.B. 2076, Yola, Adamawa State, Nigeria

Magnetic Resonance Imaging has stirred a great deal of interest in the medical community. As the image qualities are improving and as the amount of information that they can offer has been appreciated, the modality has become the primary topic of discussion among imaging scientists, imaging physicians, hospital administrators and government officials responsible for funding health care in many countries around the world. The combined effects of NMR and MRI in medical studies in human – a vast complex and very promising prospect – has not been adequately explored and are being investigated by scientists, engineers, mathematicians and clinicians around the world. Not only that such tasks are intellectually very fascinating and challenging in themselves, they are having spin-off benefits for other areas of science and technology. In this paper, we present a brief review of current efforts on the application of Nuclear Magnetic Resonance Imaging (NMRI) in human blood flow estimation with an aim to make life easier for the beginners in the field and we also hope that it will be helpful to the practitioners in the field as well.

1. Introduction

Blood is important for the proper functioning of the body and is channeled to every part of the body for proper nourishment through veins and arteries being the main server that takes away the waste products set free by living tissues. It also has the ability to repair organs.

Blood is forced through the cardiovascular system by the pressure generated by the pumping of the heart. These vessels are the arteries, highly elastic and muscular; they distribute the blood to the smaller arterioles and ultimately through thin walls of which the exchange of fluid and small molecules occurs. Blood returns to the heart through the venules and wide thin veins.

The mammalian heart is a four-chambered pump, well adapted for the separation of blood low in oxygen content, which is handled by the right side of the heart, from oxygenated blood returning from the lung to the left side of the heart, forming the pulmonary and systemic circulations.

Pulmonary circulation is a low-pressure system with low resistance to the blood flow that nevertheless must handle the same volume of blood in the same time as the systemic circulation to keep the volume of blood in the right and left sides of the heart the same [56, 2]. The left ventricle, pumping against the high resistance of the systemic circulation, is considerably more muscular and heavier than the right ventricle, which pumps against low-resistance of the pulmonary circulation.

Having a double circulation, systemic and pulmonary, the heart conveys the great advantage of permitting equal volumes of blood flow in a given time through each circulation but at very different arterial blood pressures. The mean systemic arterial blood pressure in human is 90 to 100 mmHg, whereas the pulmonary arterial pressure is only 8 to 20 mmHg. The amount of blood that passes a point at a given period of time is called blood flow rates. The blood flow rate, Q, at a point depends on the blood velocity, V, and the cross-section, Ω_P of the vessel at any point. Thus,

$$Q = V\Omega_P \tag{1}$$

It is usually expressed in milliliters or liters per minutes and also in milliliters per second. Blood flow is also expressed in other units.

The key problem of heart lies in the “fuel lines” or the blood delivery routes to the heart. Blood leaving the heart is pumped into the body through huge arteries - the aorta- while much of this blood is channeled off into the coronary arteries (arteries supplying the heart muscle). This is the means by which oxygen and nutrients are carried to all part of the heart. As a result of build-up of fatty deposits in the coronary arteries, their channels are narrowed [56, 38] a condition that is referred to as

* Corresponding author.

atherosclerosis. When the heart of a person suffering atherosclerosis needs more blood to meet some physical or emotional emergency, a small part of the heart is starved of blood, setting up an electrical pattern that upsets the beating rhythm. The heart then goes into an unusual and serious complication called ventricular fibrillation in which it switches chaotically and ineffectively, and stalls from lack of a driving force. Death of the individual occurs in a few minutes if no proper pumping action is restored. The blocking of the coronary artery is referred to as coronary thrombosis or occlusion. The result of this is heart attack, which is referred to as myocardial infarction. Many lives are being lost by this sickness all over the world today! When the blockage involves the brain nerves it results to stroke.

Apart from the blockage of blood pathways in the arteries, there are other physiological conditions of the heart resulting in irregular or abnormal flow of blood from or within the heart. These may include flow obstruction [56] due to valvular heart disease or valvular lesions or stenosis of the heart valve. A literature on the assessment of aortic regurgitation (backflow of blood) using MRI was given by Sebastian et al. [52].

From the foregoing troubles to which the heart can be subjected to, many scientists [38] are working to see how blood flow in the human vessel in every part of the body can be estimated. One such method currently in use is nuclear magnetic resonance and magnetic resonance imaging (NMR/MRI).

2. Nuclear Magnetic Resonance (NMR)

Nuclear magnetic resonance involves the absorption of radio frequency (rf) energy by nucleus having net unpaired nuclear spins and thus a nuclear magnetic moment such that the nucleus when placed in a magnetic field (B) will satisfy the condition

$$\gamma B = \omega \tag{2}$$

where, ω is the incident radio frequency, γ is the gyro-magnetic ratio of the nucleus. The radio frequency acts like a smaller magnetic field that rotates the net magnetization vector from the z-axis toward the x-y plane.

In the classical approach, when certain nuclei are placed in a magnetic field, they resonate when a particular radio-frequency power is applied (equation 2). The nuclei absorb energy from the rf. The nuclei that can be excited in this manner are those that have odd number of protons, an odd number of neutrons, or both and thus having a net magnetic moment [33]. Before the magnetic field is applied, the magnetic dipoles of the nuclei are randomly distributed mostly due to thermal effect. The application of uniform magnetic field causes the dipoles to align such that there is a net magnetization vector along the line of induction of the magnetic field. Suppose the line of induction is the z-axis. The net magnetization depends both on the magnetic field B and the temperature, T given by

$$\overline{M} = M_0 \overline{B}(x) \tag{3}$$

where $\overline{B}(x)$ is the Brillouin function and

$$x = \frac{g_N \mu_N I B}{k_B T} \tag{4}$$

$$\overline{B}(x) = \frac{2I+1}{2I}\coth\frac{2I+1}{2I}x - \frac{1}{2I}\coth\frac{x}{2I}. \tag{5}$$

where g_N is a dimensionless constant called the nuclear *g*-factor, μ_N is the magnetic moment, I is the nuclear spin quantum number, and k_B is the Boltzmann's constant. In terms of the spin number I [11],

$$M_0 = N\frac{\gamma^2 \hbar^2 B_0 I(I+1)}{3k_B T} \tag{6}$$

Measurement of this absorption phenomenon enables us to get important information about the motion of the nucleus relative to the static magnetic field [16].

Blood is a liquid where magnetic resonance effect can be very well explained. When excited by magnetic field, blood undergoes Larmor's precision motion about the magnetic field axis due to the presence of nuclear spin in it.

It is assumed that the blood or fluid protons, prior to entering the excitor coil are magnetized by a static B_0 field to an equilibrium magnetization M_0, that is given by a well known Brillouin Functions. The time dependent rF B_1 field is in the laboratory X direction which coincides with the axis of the excitor and detector coils.

The Bloch equations in the laboratory frame of axes are given by

$$\frac{dM}{dt} = \gamma(M \times B) + \text{relaxation terms} \qquad (7)$$

with

$$M = iM_x + jM_y + kM_z \qquad (8)$$

and

$$B = kB_0 + iB_1(t) \qquad (9)$$

The rF $B_1(t)$ field usually is of the form

$$B_1(t) = B_{10}\cos\omega t$$

It can be viewed as two rotary magnetic fields (rotating with angular frequency ω) and amplitude $B_{10}/2$, in clockwise and counterclockwise directions [54]. One of this does not aid rF absorption at resonance and is so discarded.

This is not even when M is not flow dependent solutions of the above equations in the laboratory frame of axes. One, therefore, resorts to a rotating frame of axes, whose z axis coincides with Z axis of the laboratory frame and x-y axes of rotating frame rotates with angular frequency ω about the x axis. The x axis of the rotating frame makes an angle ωt with the X axis in the laboratory frame. In this rotating frame $B_1(t)$ is viewed as time independent and equation (9) is written as

$$B = kB_0 + B_{10}/2$$
$$= kB_0 + iB_1'$$

and in the absence of blood flow,

$$\left(\frac{dM}{dt}\right)_{lab} = \left(\frac{dM}{dt}\right)_{rot} + (\Omega \times M)_{rot} \qquad (10)$$

where $\Omega = \omega - \gamma B_0$.

At resonance Ω = 0 and

$$\left(\frac{dM}{dt}\right)_{lab} = \left(\frac{dM}{dt}\right)_{rot} \qquad (11)$$

with, rF B_1 field, time independent in the rotating frame. When flow velocity is time independent, i.e., for steady flow velocity, V,

$$\frac{d}{dt} = \frac{\partial}{\partial t} + V.grad \qquad (12)$$

The B_1 field is time independent only when viewed from the rotating frame, which is rotating about the Z axis of the fixed laboratory frame with the angular frequency ω of the field. The axis in the latter frame coincides with the laboratory z-axis, the rotating frame x makes an angle ωt at any instant of time t with the laboratory X axis. The x,y,z components (in the rotating frame) of magnetization of a fluid bolus are then given from equations (13) to (15)

$$\frac{dM_x}{dt} = V.gradM_x + \frac{\partial M_y}{\partial t} = \frac{-M_x}{T_2} \qquad (13)$$

$$\frac{dM_y}{dt} = V.gradM_y + \frac{\partial M_y}{\partial t} = \gamma M_z B_1(x) - \frac{M_y}{T_2} \qquad (14)$$

$$\frac{dM_z}{dt} = V.gradM_z + \frac{\partial M_z}{\partial t} = -\gamma M_y B_1(x) + \frac{(M_0 - M_z)}{T_1} \qquad (15)$$

To calculate M_x, M_y and M_z, one needs to have initial boundary conditions.

An NMR signal can be in the form of pulse, called Pulse NMR, or continuous, in which case it is called Continuous Wave (CW) NMR. CW NMR signal from the living static tissue depends on the quantity and constituent of the tissue and is time dependent (except the radio frequency, rf modulation). The CW NMR signal from blood protons depends on: (i) proton content; (ii) T_2 relaxation time; (iii) its velocity; and (iv) cross-section of the blood vessel [15].

The pulsatile flow of blood adds a time dependent component to the net CW NMR signal. In order to measure the static and pulsatile flow components, one needs to develop strategies to eliminate the static tissue signal. Many researchers are using pulsed NMR techniques to estimate the blood flow. The mathematical analysis of the resulting pulsed signal is much simpler than that of the CW NMR signal, whereas the former is much more expensive than the later. Even though many researchers are engaged in developing pulsed NMR technique for estimating blood flow, the measurements could be fraught with errors if the static magnetic field is not extremely homogenous (1 part per 10^8). The less stringent condition on the homogeneity of static magnetic field makes CW NMR system promising if the complicated mathematical analysis of blood flow estimation could be theoretically tackled. Under this condition,

the CW NMR technique is expected to make a significant contribution to the medical diagnostic tools used to estimate the blood flow in humans at costs that would be affordable by the common patients suffering from various ailments arising out of disturbed blood flow.

There are other methods too to determine blood flow in the human body. For example, the ultrasonic Doppler effect method, which is used to acquire one dimensional velocity profile of the center of the blood vessel [55, 60]. The NMR technique, however, has a basic advantage of making available two-dimensional velocity profiles and moreover, the potential of measurement sites are not limited as in

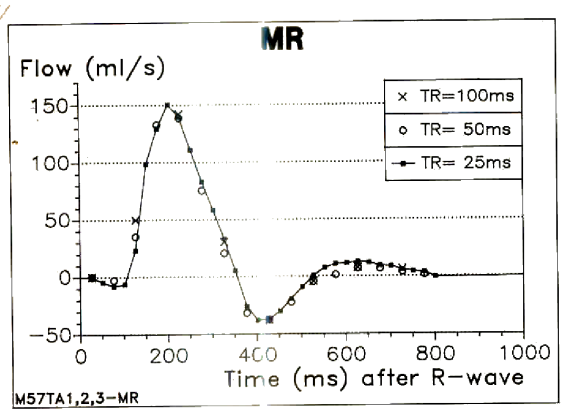

(a)

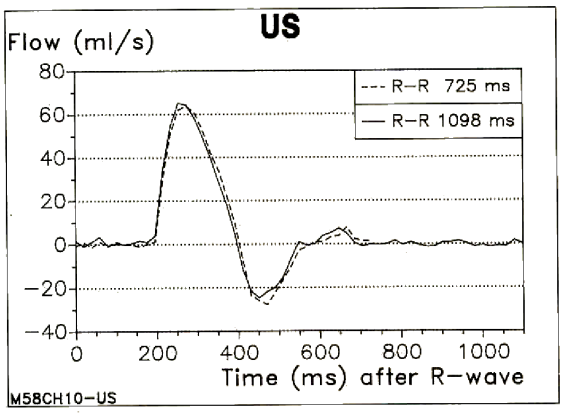

(b)

FIG. 1. (a) Temporal MR imaging flow curve of blood flow in abdominal aorta of healthy volunteers measured with different TR for 1 hour shows the physiologic reproducibility and the importance of a high sampling rate to detect fast changes of the flow. (b) Temporal flow curve of abdominal aorta in volunteer nonphasic arrhythmia of the sinus. Curve was acquired with multi-gated Doppler US during two consecutive heart beats.

Fig. 1 shows the result of measurement of blood flow in the abdominal aorta of healthy volunteers using NMR and US Doppler methods [55, 60]. This result credited MR imaging as a powerful diagnostic tool for blood flow measurement which has become very popular and seems to be fast replacing many other methods today.

Apart from being used in the measurement of blood flow in human vessels, NMR/MRI is capable of giving the image of certain tissues in the body as does X-rays. Also NMR scanning is not hazardous as X-rays and other known scanning techniques used for medical diagnosis. This makes it possible to be used repeatedly on a patient in a given time with minimal side effects, which is not possible with a technique like X-rays.

At any point in a non-invasive measurement of blood, it is important to know the cross-section of the blood vessel. The CW-NMR can give a close form relationship not only for the blood vessel cross-section but can also give strategies to estimate relevant parameters of importance like the pulsatile blood velocity, spin-lattice relaxation time, spin-spin relaxation time, and steady velocity of blood, which will give idea about the hemodynamic processes in any vessel [15].

On the whole, this review is aimed at bringing closer to us in Nigeria and Africa at large the wide growing concepts of NMR in medicine. It will create awareness for researchers in these parts of the globe as just mentioned who will want to know this fascinating and fast growing field of medicine and would make life easier for both beginners and practitioners in the field.

3. Blood Flow Estimation by NMR

The two main approaches to blood flow measurement are the invasive and non-invasive methods. Invasive measurement involves the opening of the body (a surgical procedure) before it is carried out. Non-invasive measurement on the other hand, do not involve opening of the body for estimation to take place. There is also a minimally invasive measurement [2] that involves the injection of contrast material invasive into the venous or gas transport through ingestion into the lungs. The non-invasive method obviously attracts more attention because of its advantages.

We have seen that nuclear magnetic resonance involves the absorption of radio frequency energy by nucleus having net unpaired nuclear spin and thus a nuclear magnetic moment, when the nucleus is placed in a magnetic field B and a radio-frequency, satisfies equation (2). Measurement of

this absorption phenomenon enables us to get important information about the motion of the nucleus relative to the static magnetic field as was first exhibited by the work of Suryan et al. [57]. NMR permits a fast, accurate and noninvasive measurement of blood flow and cross-sectional area of the vessels because its signal strength is extremely sensitive to these medically important parameters.

For any given magnetic field strength, the nuclei of an NMR-sensitive element can only absorb energy in response to an rf pulse of a particular frequency satisfying equation (2). The frequency of precession of nuclei about a magnetic field, B is called the Larmor frequency, ω_L. At resonance, the radio frequency ω is equal to the Larmor frequency ω_L. When the radio frequency is applied, the nuclei experiences a torque and this changes the direction of the net magnetization vector away from the direction of the static magnetic field (the z-axis) [33]. If the rf pulse is left on just long enough for the net magnetization vector to be entirely in the x-y plane and is then turned off, the net magnetization will continue in to rotate in the x-y plane, thus generating a signal. This signal is the maximum signal that the net magnetization vector can generate. This is because only its x,y component can generate a signal.

Clearly, if the vector was pointing in the + z or – z direction, no signal would be generated. When the rf pulse is turned off, signal emission begins. This implies a loss of energy from the rotating nuclei causing the precession motion of net magnetization vector to decay. Eventually, the net magnetization vector will point, once again, in the direction of the z-axis. The emitted signal diminishes accordingly.

The emission amplitude is a function of the density of the NMR-sensitive resonating nuclei present. The relaxation (decay) time has two components: longitudinal relaxation time, which is called T_1, and the other transverse relaxation time, T_2. T_1 is related to the nuclear environment of the resonating nuclei and it is thus called the spin-lattice relaxation time. It measures the rate of return of the net magnetization vector M_Z to its original value M_{Z0} along the z-axis.

$$M_Z = M_{Z0}\left(1 - e^{-\frac{t}{T_1}}\right) \tag{16}$$

For NMR of the blood flow, t = 0 may be time the first un-magnetized blood bolus enters B. Equation (16) also describes the growth of the M_Z component of the magnetization (along the applied B field direction, i.e., z-axis) through the spin-lattice relaxation time. T_1 describes how M_Z returns to its equilibrium value M_{Z0}; t is the time after the displacement of M_Z from its equilibrium value [31]. Therefore, T_1 is defined as the time required to change the z-component of the magnetization by a factor, e. T_2 is related to the spin-spin interactions (dipolar and exchange) of the resonating nuclei and is therefore called spin-spin relaxation time. It measures the de-phasing of the resonating nuclei (in the x,y plane) before they lose their absorbed energy. The decay of the transverse components, i.e., M_X, M_Y is given by

$$M_X = M_{X0}e^{-\frac{t}{T_2}} \tag{17}$$

T_2 is clearly never longer than T_1 and is often much shorter. If the static magnetic field B is switched off then M_Z decays as follows:

$$M_Z = M_{Z0}e^{-\frac{t}{T_1}} \tag{18}$$

$M_{Z0} = \overline{M}$ = Equilibrium Magnetization at a given T, given by the Brillouin function through equation (3). M_{X0} is the x-component of the magnetization after the application of rf pulse and before it starts T_2 decay. T_1 and T_2 are equally defined as the time constants of their respective (approximately) exponential decay. Thus, after three T_1's, 95% of the longitudinal decay is complete. The three parameters (nuclear density, T_1 and T_2) are sufficient to distinguish between many human tissues, from diseased to normal. The intensity of the NMR signal from the static tissue is independent of ρ_N, T_1 and T_2.

4. NMR techniques

There are many NMR scanning techniques. However, three [54, 31] of them stand out in particular: the saturation-recovery (SR) technique, inversion-recovery (IR) technique, and the spin echo (SE) techniques.

In the SR technique, a 90^o rf is applied (one that rotates the net magnetization vector by 90^o from the z axis), the transverse gradient (the "read" gradient) is then applied and data is collected. Whether a full or partial recovery is obtained depends on whether a longer or shorter time than T_1 is the waiting period before applying another 90^o rf

pulse. Tissues with nuclei having a short T_1 appears light while tissue with nuclei having long T_1 appear dark. However, flowing blood appear light. For this reason SR technique shows flowing blood and blood vessels very clearly [2].

In the IR technique, a single 180^o- rf pulse is applied and then after a period of time a 90^o-rf pulse is applied again. After the 90^o-rf pulse is shut off, "read" gradient is applied and data is collected. If T_1 is less than the waiting time, full recovery would have taken place and the 90^o pulse will leave the net magnetization vector in the x-y plane. A value of T_1 less than the waiting time gives a light appearance on the scan, while a long T_1 period appears as dark on the scan. Hence, the technique yields a mark differentiation between gray and white matter because in gray matter the protons are mostly in water, that is, they are free (short T_1) but in white matter they are usually found in lipids (longer T_1).

The SE is based on a selection of rf amplitude H_1 and pulse width t_ω to produce particular phase length such as 90^o pulse, which is

$$\gamma H_1 t_{\omega_1} = \pi / 2 \tag{19}$$

and 180^o pulse given by

$$\gamma H_1 t_{\omega_2} = \pi \tag{20}$$

An initial 90^o pulse will bend the magnetization into the x,y plane, and a subsequent series of 180^o pulses will be used to monitor the rate at which it loses coherence in this plane. The initial 180^o pulse follows the 90^o pulse by a time interval τ and the consequent pulses are separated by a time interval 2τ. The result is the appearance of a series of echoes (known as spin echoes) between the 180^o pulses, and the echoes decay with time in a manner that depends upon the relaxation times.

5. NMR/MRI spectrometer in the estimation of blood flow rates

There has been a considerable increase in the possible applications of NMR on blood flow estimation following the first demonstration by Suryan in 1951 of NMR signal changes caused by the flow of liquid through NMR spectrometer. The first known medical application of this flow phenomenon was made by R.L. Bowman in 1956 [10] at the Laboratory of Technical Development (LTD) of the National Heart, Lung and Blood Institute. Bowman and Kudravcev showed that the use of a high-level radio frequency field, B_1, enabled the desired response of increasing NMR output as a function of flow velocity to be obtained. By 1970, the first commercial magnetic resonance flow meter was manufactured by Badger Meter Inc., for measuring "hard to measure" fluids such as slurries and those with low lubricity.

With regard to the non-invasive blood flow application in humans, only occasional measurements were made and by a limited number of research laboratories. In fact, Noodergraaf in his book, Circuitry System Dynamics, published in 1978, stated that "Many years of development were yet to yield a practical instrument". Preliminary tests demonstrated that blood flow could easily be measured *in vitro* in tubing. With the continued encouragement and support of R.L. Bowman (LTD) and the technical assistance of Richard E. Halbach, and Sergio Salle-Cunha, who did their Ph.D. dissertations at MCW (through a collaborative arrangement with Marquette University), the first clinical test on human volunteers were performed in October 1975 using a limb NMR blood flow meter. The first patient was studied in November 1976.

The Badger NMR flow meter (Fig. 2) contains, among other components, a crossed coiled NMR detector and is used at a low steady field, H_oD =58.6 G, corresponding to Larmor frequency of 250 KHz. Ceramic type permanent magnets are located upstream of the detector and produce the major part of the magnetization for the flow-meter. The copper coil is used in a single-side band receiving system. A pulse current, applied to the tagger coil is used in a single-side band receiving system. A pulse current applied to the tagger coil creates a bolus of charged magnetization in the flowing liquid. The passage of this bolus through the receiver coil is detected, causing another tagger pulse to be generated by the phase comparer/integrator/vco circuitry. Either a frequency meter can be used to give the flow velocity or volumetric flow rate, or a counter can be used to indicate the total amount of the liquid flowing through the flow meter in a given time.

6. The pulsed NMR

The pulsed NMR is subdivided into the pulsed flow method and the pulsed imaging method. Pilkington et al. [45] first demonstrated the pulse flow method, in 1965 at Duke University using an "active tag" method to determine the time of flight of a bolus of fluid between an upstream tag coil and a downstream detector coil. A "180 label" i.e., a

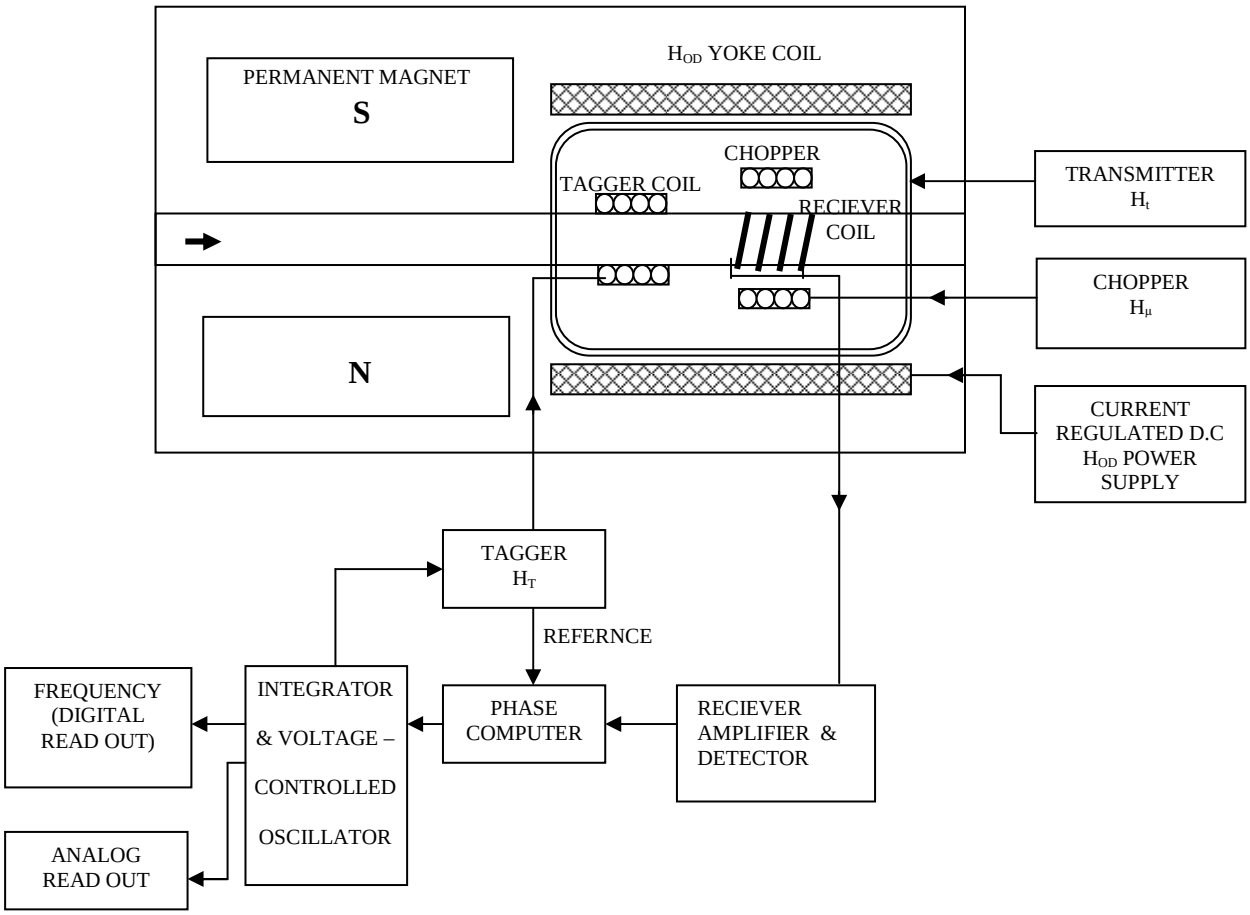

FIG. 2. Block diagram of a magnetic Resonance flow-meter manufactured by Badger Meter, Inc., Brown Deer, Winsconsin (with permission from Battocletti, J.H., Pipe Line Industry, 1968).

pulse which inverts the magnetization vector, was used as a "tag". When the "tag" was sensed at the receiver coil, another "180^o label" was applied to get the time of flight, from which flow velocity was determined. The first application of pulsed flow NMR in humans, based on the pioneering work of [26, 27], was also reported by Van et al. [58]. The rf frequency is applied in the sequence 90^o-τ-180^o-τ-180^o which is basically a spin echo sequence.

Theoretical analysis and experimental verification were conducted by Devine et al. [16] for both one coil and two-coil pulsed NMR systems. An approximate equation for the normalized signal amplitude due to flowing liquid only is given by

$$S(t) \cong e^{-\left(\frac{1}{T_2}+\frac{V}{L}\right)t} \tag{21}$$

where, V is the mean flow velocity and L is the effective length of the detector coil. The mean flow velocity is computed by means of the slope of S(t) at t = 0 using the following equation,

$$V = -L\left[\frac{1}{T_2} + \left(\frac{dS(t)}{dt}\right)_{t=0}\right] \tag{22}$$

To compute V in an experimental set up, the relaxation time T_2 must be determined. L can be determined by means of a controlled experiment

with a liquid whose T_2 is known.

7. A Theoretical work on the estimation of blood flow parameters by CW NMR technique

De [15] showed theoretically that using the method of CW NMR excitation with a separate detection system, one could virtually eliminate the problem of static signal and quantitatively estimate the pulsative and steady components of blood flow velocity and blood flow rates. Furthermore, he explained that the measurement of pulsatile components of the CW NMR signal would be erroneous without correction for steady flow velocity. He, therefore, showed a method of extraction of steady velocity, the pulsatile velocity, the spin-spin relaxation time, and the vessel cross-section.

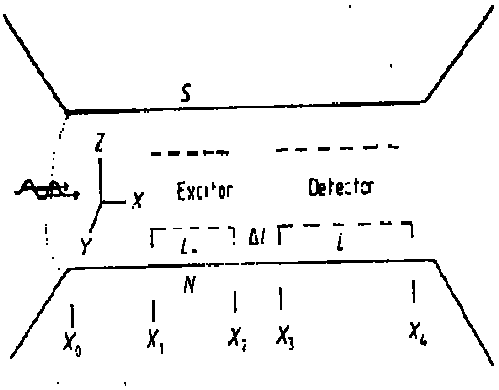

FIG. 3. Diagram of the CW NMR Excitation Scheme with Separate Movable Detection System for an accurate estimation of the steady velocity, the peak pulse velocity and the total cross-section of the blood vessel. Here, L_e is the length of the excitor coil and Δl is the separation of the excitor and the detector coil of length L.

The simple geometrical arrangement of the CW NMR system is shown in (Fig. 3). CW NMR excitation is carried out over the excitor coil of length $L_e = X_2 - X_1$. A fluid flowing in from the left is assumed to be magnetized to an equilibrium value Mo before entering the excitor coil (Fig. 3). Static tissue in the excitor coil region is also subjected to CW excitation. The B_o field inhomogeneity should be less than that of the rf B_1 field. The dependence of NMR signal on flow rate begins with a model in which B_1 is zero outside the excitation coil and constant within. Beyond the excitor coil length, a detector coil receive the signal from the blood excited in the excitor coil region, the detector coil can be positioned at different distances ΔL from the excitor coil. The signal is the result of processing transverse magnetization M_y of the flowing spins and is dependent on both the flow velocity and T_2 relaxation time.

For blood flowing with steady velocity V_0, the M_x and M_y component were separated. For a given blood bolus at any position measured from X_1 ($X_1 < X < X_2$) (Fig. 3):

$$M_x = A\left(1 - e^{-\frac{X}{V_0 T_2}}\right)\cos\left(\frac{f_0 X}{V_0}\right) \tag{23}$$

$$M_y = B\left(1 - f_0 T_2 e^{-\frac{X}{V_0 T_2}} \sin\left(\frac{f_0 X}{V_0}\right)\right) \tag{24}$$

where

$$A = \frac{\gamma f_0 M_0 B_1 T_2^{\,2}}{1 + f_0^{\,2} T_0^{\,2}} \tag{25}$$

$$B = \frac{f_0 B_1 T_2}{1 + f_0\, T_2^{\,2}} \tag{26}$$

Finally, when the signal I_{fs} is modulated and detected with reference to the same rf B_1 (phase sensitive detection), the signal is expressed as

$$I_{fs}(V) = CQ_s\left[e^{-\frac{\Delta L}{V_0 T_2}} - e^{-\frac{(L+\Delta L)}{V_0 T_2}}\right] \tag{27}$$

Here, $C = B\omega\, T_2 \cos\phi$, and ϕ is the given phase introduced in the phase sensitive detection. $Q_S = \beta V_0$ is the steady volume few rate.

The signal for the pulsatile flow rate is

$$I_{fs}(t) = C_0 V_{(t)}\left[e^{-\frac{\Delta L}{V(t) T_2}} - e^{-\frac{(\Delta L + L)}{V(t) T_2}}\right] \tag{28}$$

where $C_0 = k\beta c'$ and c' is the instrumental factor. V(t) is given by

$$V(t) = V_0 + V_{pulse}(t) \tag{29}$$

$$V_{pulse}(t) = \frac{V_{pulse}^{0}}{0.365} e^{-4t} \sin(-15\pi t) \tag{30}$$

From the analysis, however, in order to measure the steady flow rate, the signal must be

obtained for three small values of ΔL (L is the length of detector coil), ΔL is the separation between the detector and the excitor coils (Fig. 3). Then, the static tissue signal can be eliminated and both the steady flow velocity "V_0" and the flow rate can be obtained, as well as the pulsatile amplitude, V^0_{Pulse}. The time dependent CW NMR signals were found to be linearly dependent on pulsatile velocity only when $L_e > 40$cm, for $T_2 = 0.15$s and $L > 50$cm for $T_2 = 0.35$sec used with $\Delta L = 0$. With small excitor detector coils, it is possible by this method also to determine independently and uniquely T_2, V_0, V^0 pulse and the total cross section area of the blood vessels when both steady and pulsatile flows are simultaneously present.

8. Nuclear magnetic resonance imaging (MRI)

There are two quite distinct applications of magnetic resonance imaging where an understanding of the flow and the motion effects are important. The first is the classical examination of physiological details, where it is desirable for the relative intensity in each pixel to reflect T_1, T_2 or density value of the local material. Patient movement over the period of data collection can generate phase shifts and amplitude modulation of the magnetization vector that results in spurious intensities known as artifacts [43]. However, there are methods that were developed to eliminate these artifacts [41]. Removal of artifacts from true image is essential for accurate diagnostic procedures.

The second application of MRI in the study of flow and motion effects addresses the question of extracting both qualitative and quantitative information on blood flow from the MRI signal [25, 20]. The method is different from that of CW and pulsed NMR techniques discussed earlier. The time dependence and spatial variation of the velocity of blood flow is clinically useful as an indicator of physiological disfunction [12]. Saloner et al. [49] discussed a sequence aimed at providing a quantitative measure of blood flow in the body vessel while simultaneously suppressing the contribution of signal from stationary tissues and other materials. In the described scheme, both the tip angle of excitation α and 180° rf pulses are slice-selective with the slice thickness being along the z-direction. The longitudinal magnetization immediately preceding the α pulse after the nth such excitation cycle will attain a dynamic equilibrium given by

$$M_{11}^{n} = M_{11}^{Dyn} + \left(M_{Z0} - M_{11}^{Dyn}\right)R^{n} \qquad (31)$$

where

$$M_{11}^{Dyn} = \frac{M_{Z0}\left(1 - 2e^{-\frac{T_R - \frac{T_E}{2}}{T_1}} + e^{-\frac{T_R}{T_1}}\right)}{1 - \cos\alpha e^{-\frac{T_E}{T_1}}} \qquad (32)$$

and

$R^n = -\cos\alpha e^{-\frac{T_R}{T_1}}$, T_R = sequence repetition time and T_E = echo time.

It is assumed that all transverse magnetization remaining after data read out interval n-1 has either decayed to zero through irreversible T_2 decay or has been eliminated by a suitable spoiler gradient encoding. The most important diagnostic factor in MRI is the contrast to noise ratio (CNR) i.e., the difference in signal intensity normalized to the image r.m.s noise level for two special regions of interest ROI (lesion, tumor, cyst, hemorrhage etc.) and the normal, healthy adjacent tissue within the same organ (brain, spinal cord, liver, muscle etc). The intrinsic tissue parameters depend on the motion of the nuclei, the temperature, the viscosity of blood, and the magnetic effect of nearby nuclei [1]. Therefore, since they depend on the local tissue conditions, they are bound to carry information about the disease state of tissue [3, 4]. The pioneering work of blood flow measurement and detection of atherosclerotic disease using NMR imagers was made at the University of California at San Francisco (UCSF) beginning 1981.

The "transit time" method was first proposed by Crooks et al. [14] and later developed by Wherli et al. [66] (and Singer and Crooks [53]) named as the "Selective Saturation-recovery Spin Echo Method". He derived an equation to remove the effect of stationary spin signals by means of spin echo detection modality i.e., the 90°-TE/2-180° sequence given as:

$$S(T_1) = S_0\left[\frac{VT_1}{d} + \left(\left|\frac{d - VT_1}{d}\right|\right)\left(1 - e^{-\frac{T_1}{T_2}}\right)\right]\left(1 - \frac{VT_1}{2d}\right)e^{-\frac{TE}{T_2}} \qquad (33)$$

where, T_1 is the elapsed time between the randomization of spin and the 90° rf pulse of the spin echo sequence. TE/2 is the time between the 90° and 180° pulses and T_2 is the transverse

relaxation time. S_0 is the signal intensity when $VT_1 = d$ exclusive of the decrease in signal occurring during this time TE. Equation (33) is only applicable for $T_1 \leq d/V$.

Grover [24] developed the phase encoding method of blood flow measurement in one dimension at the University of California at Berkeley. In this development:

(a) The amplitude of spin echo is given by

$$A(2\tau) = \int_{-\pi}^{\pi} g(\Phi) e^{-j\Phi} d\Phi \tag{34}$$

where, π is the spin echo delay time. If g(Φ), the distribution of the spin echo signal, is an even function, then $e^{-j\Phi}$ is replaced by;

(b) The phase shift is given by

$$\Phi = \gamma G V \tau^2 \tag{35}$$

where, G is the slice selection gradient in the direction of the velocity V;

(c) Equation (34) then takes the form

$$A(2\tau) = \int_{-\infty}^{\infty} f(V) e^{-\gamma G V \tau^2} dV \tag{36}$$

where, $f(V)$, is the velocity distribution function;

(d) Equation (36) has the form of Fourier transform of $f(V)$. Therefore, $f(V)$ has the form

$$f(V) = \frac{1}{2} \int_{-\infty}^{\infty} A(2\tau) e^{-i\gamma G V \tau^2} d\tau^2 \tag{37}$$

In actual experiment, either G or τ in equation (37) is varied in discrete steps to obtain a matrix of values for $A(2\tau)$. The Fourier transform of this matrix then yields the velocity distribution function, $f(V)$. This technique was demonstrated by Grover and Singer [24] for laminar flow in tubes and for blood flow in a rat tail and human finger.

The main shortcoming of this method is the time required to formulate the matrix in two dimensions, where some semblance of an image can be obtained; the calibration capability is also uncertain.

9. MRI image formation for human blood quantification based on two-dimensional Fourier transform: 2D-FT (idea behind the slice selection method)

When a patient is placed in MRI scanner with homogenous magnetic field B, nuclei with magnetic moment μ aligned parallel to, and precess around, the main axis of the applied magnetic field. They will be excited if a radio frequency pulse is applied through a coil perpendicular to the magnetic field at the proton Larmor frequency.

However, to examine a specific slice only, a second magnetic field that changes linearly with position is superimposed on the main static field [5, 7, 59]. The resulting magnetic field is according to the equation

$$B(\vec{r},t) = B_0 + \vec{r}(t) G(\vec{r},t) \tag{38}$$

The magnetic field gradient is therefore stronger or weaker in some places than in the others. In the patient, e.g., the magnetic field strength increases for different cross-sections from the feet towards the head. Consequently, the protons in the different slices experience different magnetic fields and thus have different precession frequencies. The rF pulse that excites protons in different slices must have a specific bandwidth. If this gradient is oriented from head-to-toe of a patient, then every transverse slice in the patient resonates at different Larmor frequencies. If the patient is then exposed to a radio frequency pulse with a narrow range of frequencies (a narrow bandwidth), then only those nuclei in the slice where the Larmor frequencies match the frequencies of the rF pulse actually absorb the rF energy. This process is called slice selective excitation and the gradient, which enables us to examine a specific slice, is called the slice selection gradient.

The magnetic field gradient necessary for slice selection is relatively small compared to the main magnetic field, since the absorption of rF energy by precessing nuclei occurs at the Larmor frequency. The direction of the magnetic gradient is perpendicular to the slice orientation. The slice thickness is controlled by both the amplitude of the magnetic field gradient and the bandwidth of the rF pulse. The slice profile and the pulse shape are each other's Fourier's transform. Under the influence of the magnetic field gradient, spins across the thickness of the selected slice will precess with slightly varying frequencies i.e.,

$$\omega = \gamma B + \Delta\omega = \gamma B + G_z Z \qquad (39)$$

Therefore, the selected spin will diphase (that is spread out). For maximum signal, the spin in the selected slice must be brought back into phase. This is accomplished through the use of a spin-rephrasing gradient, which is simply a field gradient of opposite polarity from the initial slice selection gradient. The gradient creates phase coherence among the nuclei in the selected slice.

If a second field gradient G_X is applied orthogonal to the slice selection gradient while receiving the signal, the frequency of the emitted signal changes according to its position along the G_X axis. The signal in the centerline (isocentre) alone continues to precess at the original frequency. Therefore, G_X provides spatial information along one axis of an image slice.

A third gradient G_Y can then be applied at time t = 0 before and orthogonal to G_X while G_X is fixed. The spins will have their resonance frequency, and hence their rate of precision altered according to their position along the y-axis. As soon as the phase encoding gradient is switched off, spins at different points along the y-axis again begins to precess at the same frequency, but with different phases depending on their relative position along the y-axis.

There are several other methods that can be used to produce an MRI image.

(1) A commonly used method in every day clinical practice is the spin warp technique [17], which is an improvement over the two-dimensional Fourier transform (2DFT) imaging idea. The first pulse has spatial profile and is applied in the presence of a magnetic field gradient along the axis, perpendicular to the desired image plane (slice selective gradient Gz). If the rf pulse is tailored so that its FT is rectangular, only spins with resonance frequency with the interval τ centered at ω_0 will irradiated. When this irradiation occurs in the presence of a magnetic field gradient (MFG) oriented along the z-direction, a slice of thickness

$$d = \frac{\nabla\omega}{G_z\gamma} \qquad (40)$$

where, γ, the gyro-magnetic ratio will be irradiated.

(2) The saturation recovery (SR) protocol [24] is very similar to the basic spin warp sequence except that a selective π pulse is used to allow for multi-slice data selection in a short time. This allows for data acquisition of multiple slices in greatly reduced time and is now common practice in MRI. The theoretical pixel signal intensity for an SR sequence [24] is given by:

$$S = M_{Z0}\sin\alpha e^{-\frac{TE}{2T_2}}\left[1+e^{-\frac{TE}{2T_2}}-e^{-\frac{TE}{2T_1}}+\cos\beta\right]$$
$$\cdot\left[e^{-\frac{TE}{2T_1}}-1\right]e^{-\frac{TE}{T_1}}\left[1-\cos(\beta-\alpha)e^{\left(-\frac{TE}{2T_1}-\frac{TE}{2T_2}-\frac{TE}{T_1}\right)}\right] \qquad (41)$$

where T_1 is the local spin-lattice relaxation time, T_2 is the local spin-spin relaxation, *TE* is the echo time (counted from the beginning of the sequence to the maximum of the echo signal), *TR* is the sequence repetition time, α is the tip angle of the first excitation (usually close to $\pi/2$ and β is the tip angle of the second rf pulses (close to π).

(3) For the inversion recovery (IR) protocol [24], all the rf pulses are applied in slice selective mode to allow for multi-slice data collection as described for the SR protocol. The pixel intensity in this case is equal to:

$$S = \frac{M_{Z0}\sin\alpha\, e^{-\frac{TE}{T_2}}\left[1+(\cos\beta-1)e^{-\frac{T_2}{T_1}}-\cos\beta e^{-\frac{TR}{T_1}}\right]}{1+\cos\beta\cos\alpha e^{-\frac{TR}{T_1}}} \qquad (42)$$

where, all the variables are the same as in the SR case. Generally, the IR protocol is more difficult to apply in standard clinical practice, mainly because of various problems with phase correction and increased imaged noise that occurs when, T_1 is chosen to produce small signals.

10. Modified stimulated echo sequence for elimination of static signal from stationary materials (MSTE)

Vessel imaging has a very exciting prospect for magnetic resonance application in medicine. The main problem is to image uniquely the moving blood in veins and arteries and to eliminate the surrounding tissues [9]. A basic cancellation excitation consists of introducing a bipolar gradient between two 90° radio frequency pulses as a supplementary preparation period of the imaging sequence. A technique that is able to give the image of blood flow involves several or, at least, three radio frequency pulses. The same is true for 90°-t-180°-2t-180°-t (echo) with bipolar gradient modulation (BPGM) [43]. Thus, if the slice selected by the first radio frequency pulse differs from the slice determined by the third pulse, one obtains a time-of-flight method for visualization of flow passing through consecutive slices.

Another method [43], the modified stimulated echo sequence for elimination of signal from stationary spins in MRI, is still based on stimulated echo sequence. Bipolar gradient, aligned with the direction of flow, is applied during the second interval of time of the stimulated echo sequence. This provides a velocity – to – signal amplitude conversion and a noticeable diminution of signal from stationary nuclei can be obtained. A modified stimulated echo (MSTE) is generated when a 180°-radio frequency pulse is applied between the two 90° - pulses.

The variation of the echo amplitude depends on the relative spin lattice T_1 and spin – spin (T_2) relaxation times. For $T_1 = T_2$, the MSTE amplitude will be twice the usual stimulated echo (STE) amplitude and the MSTE amplitude will be zero considering new nuclei moving perpendicular to the observed slice. The phase shift at each nucleus is then related to its velocity V by [40]

$$\Phi = \gamma G V_\tau \left(\tau - \tau'\right) \tag{43}$$

where, γ is the gyro-magnetic ratio and G is the bipolar gradient. This phase shift alters transverse components of each magnetization during the application of the 180° pulse.

11. Time of flight method of measuring flow velocity

Leon et al. [35] presented a new time–of–flight method for direct imaging of flow velocities by magnetic resonance. The technique uses selective exciting and refocusing of pulses to selectively effect planes oriented in orthogonal direction in space, with the region of excitation perpendicular to the flow and refocusing region parallel to and including the flow. Both laminar and non–laminar velocity distributions are possible.

The basic idea of the method is to use a selective 90° pulse to excite a region at right angles to the direction of flow. At time after TE/2, a selective 180° pulse is used to influence a region parallel to the flow and the flow (i.e., orthogonal to the 90° pulse). The 180° pulse is made selective in order to eliminate signal from stationary spin in overlying regions and thus reduce dynamic range in the image.

12. Artifacts from pulsatile flow in MR imaging

When blood flows slowly in a vessel imaged in a conventional magnetic resonance (MR) scan, it can appear relatively “bright” against background structure. This has been attributed to the effect of a “fresh” spin inflow and blood’s long T_2 [27, 28]. As the flow rate in the vessel increases, these imaged intensities increase to maximum (the so called “paradoxical enhancement”), and then decrease towards the zero signal. This attenuation effect has been pointed to a phase – blurring phenomenon occurring in the regions of high spatial rates of change of blood velocity [64] and [65].

An intermittent observation is that one sometimes finds a pattern of distinct “ghost” images lying close to smaller vessel (usually arteries) that are bright in slow flow [22, 7]. These flow artifacts appear as “dark ghost” within the vessels and as “bright ghost” outside the vessel. Flow artifacts may cause serious confusion in the interpretation of a chemical MR image. These flows induced ghosts appear in places where there should be nothing and also come and go without reproduction depending on minor and seemingly irrelevant changes in scan sequence parameters, and sometimes even with no changes [20, 5]. It seems plausible to attribute these ghosts to physical displacements of the vessel driven by the cardiac cycle.

Similar artifacts are common annoyance due to patient motions during scan, especially those generated from the beating heart or from breathing [14, 19, 23]. In detail, these amplitudes of motion artifacts tend to propagate in the direction of the discrete phase – encoding gradient and dark structure within the patient. The pulsatile flow

artifacts appear dominated by a dark central structure and have stronger appearance close to the "moving vessel" that generates them.

Magnetic resonance imaging offers the possibility of non-invasive visualization and quantification of blood flow in many large human arteries and veins [7]. However, the assessment of complex blood flow patterns with conventional gradient echo flow sequences forms severe image artifacts. The motion of nuclear spin also influences the MRI signals by two different effects: on one hand the motion modifies the signal amplitudes and thus the brightness of vessels with flowing blood. On the other hand, the motion along magnetic field gradients modulates the phase of the MRI signal [6]. Often the two effects can cause unwanted image artifacts. However, they can be used for assessment of motion structures or organ within the human body. Because the two effects modify either the amplitude of the signal or its phase, procedures making use of these effects are either called amplitude contrast procedures or phase contrast procedures.

The amplitude contrast effects can be studied using the two modalities: the saturation recovery and the spin echo modalities. If, for instance, we consider the saturation recovery technique, a slice of thickness Δz orthogonal to the z-axis and a vessel with flowing blood passing through it in the z-direction (Fig. 4), the nuclei of the slice are excited repeatedly by 90° pulses with a repetition time T_R.

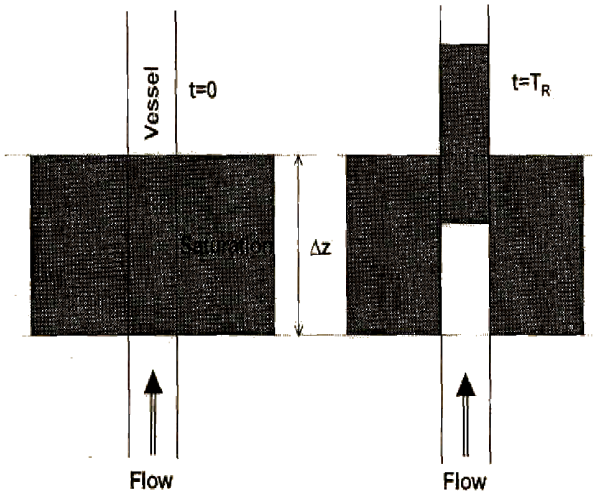

FIG. 4. Dependence of the signal amplitude on flow velocity for partial blood saturation in a vessel passing orthogonal through the slice.

Thus, the magnetization of tissue as well as that of the blood become partially saturated and recover with the corresponding relaxation time T_1 of the tissue and the blood. If the blood within the vessel moves with uniform velocity ν through the imaging plane between repetitive excitations, the nuclei within the slice will partially be replaced by "fresh" nuclei, which have not been previously excited by the rf pulses because they come from outside the excited slice or volume. The replaced spins are unsaturated and produce full signal, which may be considerably enhanced, compared to that of the surrounding tissue [6]. The amplitude of the enhanced signal σ_{PS}^{flow} depends on many factors and can be calculated according to geometrical consideration as:

$$\sigma_{PS}^{flow}\left(v,\Delta z,T_R,T_1\right)\propto\left(\Delta z-vT_R\right)\left[1-e^{-\frac{T_R}{T_1}}\right]+vT_R \tag{44}$$

Maximum signal amplitude occur when flow velocity v is sufficiently high so that during the interval T_R all spins of the slice within the vessel are replaced by unsaturated spins, i.e. when $v\geq\Delta z/T_R$

If for image acquisition the spin echo sequences are used, then the dependence of the signal amplitude on the flow velocity becomes more complicated. In addition to the signal enhancement by the inflow of unsaturated spins, between the slice selective excitation and the refocusing of echo pulses, an outflow of excited spins occur. The out flowing spins are replaced by unexcited spins, which do not form an echo after the 180° pulse and therefore do not contribute to the echo signal. A signal reduction occurs by a factor $(1-T_E v/2\Delta z)$ and should be taken into account. Considering both effects, i.e., the inflow of unsaturated spins between the repetitive excitation and the outflow between the excitation and the echo formation pulse, the amplitude of the echo signal becomes

$$\sigma_{SE}^{flow}\left(v,\Delta z,T_R,T_E,T_1,T_2\right)=\sigma_{Ps}^{flow}\left(1-T_E v/2\Delta z\right)e^{-\frac{T_E}{T_2}} \tag{45}$$

This formula is valid for $v\leq\Delta z/T_R$ and $0\leq v\leq 2\Delta z/T_E$.

The phase contrasts effects [7, 6] explain that if

spins move between excitation and signal detection along a magnetic field gradient, then they "feel" during that time a magnetic field that changes according to their spatial coordinate. As a consequence, the magnetization will progressively precess faster if moving along a gradient of increasing B, or slower if moving into the opposite direction (i.e., decreasing B). The acquired signal shows a modified phase angle as compared to stationary spins, which remain at the same location and experience constant field strength.

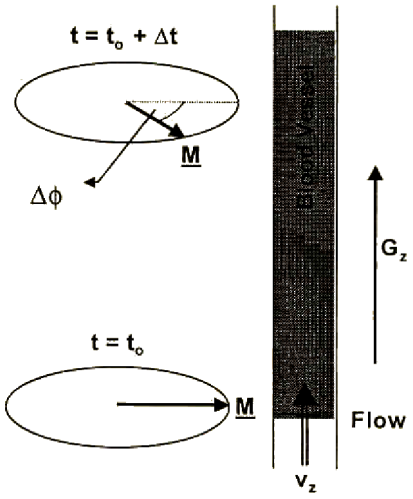

FIG. 5. Induction of a phase shift $\Delta\phi$ by the motion of magnetization along a gradient G_z.

Assuming a constant flow velocity v_z along a gradient G_z (Fig. 5), the phase angle difference $\Delta\phi$ into that of stationary magnetization can be calculated by

$$\Delta\phi = \gamma v_z \int G_z(t) t dt \tag{46}$$

The integration has to be performed over the entire time between the spin excitation and signal acquisition during which the gradient is switch on. If the time course and the amplitude gradient are known, from $\Delta\phi$ the flow velocity distribution over the vessel lumen can be determined pixel-wise from the phase images. The phase $\phi(r, T_E)$ of the measured signal is given by

$$\phi(\underline{r}, T_E) = \int_0^{T_E} \omega(\underline{r}, t) dt$$
$$= \gamma \int_0^{T_E} B(\underline{r}, t) dt$$
$$= \gamma \int_0^{T_E} [B_0(\underline{r}) + \underline{r}(t)\underline{G}(t)] dt \tag{47}$$

$$\phi(\underline{r}, t) = \gamma \underline{B}_0(\underline{r}_0) T_E + \gamma \underline{r}_0 \int_0^{T_E} \underline{G}(t) dt + \gamma \underline{v}_0 \int_0^{T_E} \underline{G}(t) t dt$$
$$+ \frac{1}{2} \gamma \underline{a}_0 \int_0^{T_E} \underline{G}(t) t^2 dt$$
$$+ \text{Higher order terms.} \tag{48}$$

where, $\underline{r}_0 = \underline{r}(t = 0)$ is the position of spins,

$\underline{v}_0 = d\underline{r}/d\big|_0 = \underline{v}(t = 0)$ is the blood flow velocity;

and $\underline{a}_0 = d^2\underline{r}/dt^2\big|_0 = \underline{a}(t = 0)$ is the blood flow acceleration.

The first term of equation (48) is constant and is induced by the static magnetic field. The second term comprises the phase values induced by the gradient field components, which are used for spatial localization. The third term is the velocity term; its value is determined by the velocity components of the blood or moving tissue. The next terms contain phase contributions induced by the acceleration and higher motion terms.

Equation (48) can be recognized that for conventional imaging of anatomical structures flow induced phase shifts and may be reduced by shortening the echo time T_E. Botner et al. [7] using a carotid bifurcation model showed that with the help of numerical simulations the accuracy of partial echo blood flow measurements seems to be sufficient in greater vessels even if the acceleration reaches values up to 50 cm/s^2.

13. Flow measurement in coronary artery

Several investigations have recently reported methods of measuring velocity and flow in coronary arteries using magnetic resonance data. These include an inflow technique, a phase difference (PD) technique [18], and a bolus tracking technique [13]. To obtain accurate flow measurement in the coronary arteries, it is

necessary to separate the motion of the blood from the motion of the vessel; this was first noted by Schiedeger et al. [50] at the Institute of Biomedical Engineering and Medical Information University of Zurich and E TH, Zurich, Switzerland. He used a separate temporary resolved 3D acquisition to estimate the myocardial velocity. This velocity estimate was then used to correct phase difference flow measurements calculated from phase–contrast acquisition.

An echo planner in-flow method was also used in which a slab is saturated and then following a short delay, a thinner slice within the slab is imaged. By collecting numerous images, each one with a different delay between saturation and acquisition, the signal versus the delay curve can be used to determine the blood velocity (assuming the flow is laminar).

In 1996, Jason et al. [32] performed computer simulation and phanton experiments to evaluate the effect of through plane motion on flow measurements obtained using PD and CD techniques. Based on the results from several volunteers, it was found that through-plane myocardial motion is often of the order of 10 cm/s during systole. Though both PD and CD techniques sustained errors, based on the myocardial velocity estimates available from the same images that provide the flow estimates, it is possible to correct the PD and CD results for through-plane motion. In PD method, the correction involves a simple addition or subtraction of the myocardial phase from the reconstructed image. In CD method, the correction involves using the same myocardial velocity information to perform a rotation of the complex image data before calculating the CD.

Although MR images of coronary arteries may eventually become useful in the visual assessment of the lesion significance, it is more likely that these images will have their greatest utility on providing flow information that may be difficult to obtain even with other more invasive method [2].

14. Quantification of blood flow in brain tumors and stroke management using MRI (more recent developments)

Following the encouraging results of clinical recombinant tissue plasminogen activator (rt-PA) treatment trials, thromblysis is increasingly used to treat acute ischemic stroke. However, because of the risk of intra-cerebral bleedings compared with untreated stroke, careful pre-treatment screening is mandatory to exclude patients who cannot be expected to benefit from this therapy. At present, this is mainly done on an empirical time-window basis. By comparing the outcome after different delays, evidence has been provided that the benefit of therapeutic vessel re-canalization exceeds the risk of bleeding and not only when therapy is initiated within three hours after the onset of stroke [37].

Permanent or transient focal ischemia caused by photo-thrombosis [51], thread occlusion [42], and thromboembolism [8, 21] have been extensively studied by taking the advantage of established magnetic resonance (MR) methods like perfusion-weighted imaging (PWI), diffusion-weighted imaging (DWI), and T_2-weighted imaging [30].

Though some of these methods listed above have yielded exciting results in rodents, a reliable prediction of individual outcome was not possible [46] because of the contrast agents, which heavily influences the magnetic properties of the tissue. However, a contrast-agent free angiographic methods like the time-of-flight (TOF) technique that detects the motion of water protons of inflowing blood by taking advantage of the intrinsic contrast with the saturated stationary tissue signal has been presented by Hilger et al. [29].

The fast growing techniques in magnetic resonance imaging has made it possible to study dynamical process of blood in the brain. Warmuth et al. [62] carried out some work to quantify blood flow in the human brain of thirty-six patient with histological proven brain tumors examined at 1.5 T. He compared the results of an arterial spin labeling and dynamic susceptibility-weighted contrast MR imaging for the evaluation of tumor blood flow in the patients. The result was a close linear correlation between the two in the tumor region of interest.

Diffusion-weighted magnetic resonance (MR) imaging and perfusion MR imaging are other advanced techniques which provide information not available from conventional MR imaging [47]. In particular, these techniques have a number of applications with regard to characterization of tumors and assessment of tumor response therapy. The fundamental principles of these MR methods and how they are being used to characterize tumors by helping to distinguish types, assess grade, and attempt to determine tumor margins have been explained by [47, 48]. The role of the techniques for evaluating response to tumor therapy is also outlined in these papers.

The search for better performance of the methods in assessing the brain tumor has resulted in other recent works [63, 34, 44, 67, 61, 39, 36].

These reports listed here show the rapid development accompanying NMR and MRI technology which every medical expert especially in developing countries are encouraged to understand.

15. Conclusion

Methods of Nuclear Magnetic Resonance and Magnetic Resonance Imaging have become very useful in medical sciences. Image qualities, which other methods of medical diagnosis (such as x-rays, ultrasound, PET) cannot produce, are being achieved through these fast growing methods. Blood flow estimation in veins and arteries and hemodynamic process in the cardio-vascular system are being simplified through the application of NMR. With the growing interest of scientists, engineers, mathematicians, and clinician in this area of study, there is not only going to be breakthrough in the medical sciences but also there will be benefits for other areas of science and technology.

Acknowledgments

We are highly grateful to and acknowledge the assistance of Prof Peter Boesiger of Institute of Biomedical Engineering, University of Zurich and Swiss Federal Institute of Technology for providing many of the materials used for this work. We also acknowledge the authority of the Federal University of Technology, Yola, Nigeria, for granting one of the authors a study fellowship in this field of study.

References

[1] A. Abragam, *The Principle of Nuclear Magnetism* (Oxford University Press, London, 1961) p.56.

[2] O. B. Awojoyogbe, "Studies on the Application of Nuclear Magnetic Resonance (NMR, MRI) in the Estimation of Human Blood Flow Rates". Ph.D Thesis (1997), Federal University of Technology, Minna, Nigeria (unpublished).

[3] J. H. Battocletti, A. Sauce Jr., S.J. Larson, S. M. Evans, R. L. Bowman, V. Kudravce, and R. E. Halback, *Biological and Clinical Effects of Low - Frequency Magnetic and Electric Fields* (C.C Thomas, Springfield, Illinois, 1974) p.263.

[4] J. H. Battocletti, A. Sauce Jr., S. J. Larson, S. M. Evans, R. L. Bowman, J. H. Lineham, V. Kudravce, W. K. Genthe, R. E. Hallouck, and F. Antionich, *Flow: Its Measurement and Control in Science and Industry.* Vol.1 "Instrument Society of American, Pittsburgh", pt. **3**, 1401 (1974).

[5] P. Boesiger, S. E. Maier, L. Kecheng, M. B. Scheidegger, and D. Meir, J. Biomechanics. Vol 25, **1**, 55 (1992).

[6] P. Boesiger and D. Meier, "Magnetic Resonance Imaging and Spectroscopy". International Zurich Magnetic Resonance Education Centre, 41 (2001).

[7] R. Botnar, M. B. Scheidegger, and P. Boesiger, Technology and Health Care **4,** 97 (1996).

[8] G. Brinker, C. Franke, M. Hoehn, U. Uhleenkuken, and K-A. Hossmann, NMR Biomed. **14**, 289 (1999).

[9] R. A. Brooks, J. N. Battocletti, A. Sances Jr., S. J. Larson, R. L. Bowman, and V. Kudracev, IEEE Trans. Biomed. Engin. BME **22** (1), 12 (1975).

[10] R. L. Bowman and V.O. Kudravcev, IRE Trans. Med. Electron, Med. **6**, 267 (1959).

[11] D. Canet, *Nuclear Magnetic Resonance: Concepts and Methods* (John Wiley & Sons Ltd., England, 1996).

[12] C. G. Carol, T. J. Padle, R. C. Schroter, and W. A. Seed, *The Mechanics of Circulation* (Oxford University Press, Oxford, 1978).

[13] D. Chien, D. Saloner, and C. Anderson, "Breath-Hold Velocity Measurement of Coronary Arteries by Bolus Tagging with Segmented Acquisition" in: Proceedings of the Society of Magnetic Resonance in Medicine. Berkeley, Calf. Society Magnetic Resonance in Medicine, 373 (1994).

[14] L. Crooks, B. Barker, and H. Chang, "Strategies for Gated MRI of the Heart" in: Program of the third annual meeting of the Society of Magnetic Resonance in Medicine. New York. Society of Magnetic Resonance in Medicine, 171 (1984).

[15] D. K. De, Phys. Med. Biol., Vol **35**, No.2, 197 (1990).

[16] R. A. B. Devine, L. P. Clark, S. Vaughn, and A. N. Serafinin, J. Nucl. Med. **23**, 1020 (1982).

[17] W. A. Edelstein, J. M. S. Hutchison, G. Hohnson, and J. Redpath, Phys, Med. Biol. **25**, 751 (1980).

[18] R. L. W. Edelman, JMRI **3**: 699 (1993).

[19] R. I. Ehman, M. T. Mc Namara, M. Pallack, and C. B. Higgins, "Respiratory Gated MRI: Evaluation of Technical Approaches" in: Program of the Third Annual Meeting of the

Society of Magnetic Resonance in Medicine. New York. Society of Magnetic Resonance in Medicine, 210 (1984).
[20] D. A. Feinberg, L. Crooks, J. Hoenninger, M. Arakawa, and J. Watts, Radiology **153**, 177 (1984).
[21] C. Franke, G. Brinker, F. Pillekamp, and M. Hoehn, J. Cereb Blood Flow Metab. **20**, 583 (2000).
[22] C. R. George et al., Ann Radiology (Paris) **27**, 405 (1984).
[23] M. W. Groch, D. A. Turner, and J. Clark, "Clinical Application of Respiratory Gating in Magnetic Resonance Imaging" in: Program of the third annual meeting of the Society of Magnetic Resonance in Medicine. New York. Society of Magnetic Resonance in Medicine, 279 (1984).
[24] T. Grover, and J. R. Singer, J. Appl. Phys. **42** (3), 938 (1971).
[25] G. Gullberg, F. W. Wehrli, A. Chimakawa J. R. Macfall, L. Axwl, and W. Perman, J. Comput. Assist. Tomogr. **9**, 537 (1985).
[26] M. A. Hemminga, P. A. de Jager, and A. Sonneveld, J. Mag. Res. **27**, 359 (1977).
[27] M. A. Hemminga, P. A. de Jager, and A. Sonneveld, J. Mag. Res. **27**, 359 (1980).
[28] M. A. Hemminga, P. A. de Jager, and A. Sonneveld, J. Mag. Res. **37**, 1 (1980).
[29] T. Hilger, F. Niessen, M. Diedenhofen, K-A. Hossmann, and M. Hoehn, Journal of Cerebral Blood Flow & Metabolism **22**, 652 (2001).
[30] M. Hoehn, K. Niclay, C. Franke, and B. van der Sanden, J. Mag. Res. Imaging **14**, 491 (2001).
[31] J. P. Hornak, (2004), "The Basics of NMR". (http://www.cis.rit.edu/htbooks/nmr), chapters 3 and 6.
[32] A. P. Jason, R. K. Frank, L. W. Kristin, M. G. Thomas, F. Richard, C.P. Dana, and A. M. Charles, JMRI **I**, 13 (1996).
[33] V. O. Kudravcev, "Liquid Flow Velocity Measurement by NMR Magnetic Labeling Technique", Paper No 21A4, Proc 1st Annual Conference Eng. Med Biol and Bio., Huston (1968).
[34] M. Law, R. Young, J. Babb, M. Rad, D. Sasaki, D. Zagzag, and G. Johnson, AJNR Am. J. Neuroradiol. **27**(9), 1975 (2006).
[35] A. Leon, S. Ann, and M. A. James, Mag. Reson Imag. **4**, 99 (1986).
[36] C. Manka, F. Traber, J. Gleseke, H. H. Schild, and C. K. Kuhl, Radiology **234**(3), 869 (2005).
[37] J. R. Marler, T. Brott, J. Broderick, R. M. Kothari, W. Barsan, T. Tomsick, J. Spilker, R. Miller, L. Sauerbeck, J. Jarell, J. Kelly, and Perkins et al., N Engl J Med. **33**, 1581 (1995).
[38] G. C. E. Mbah, Global J. Mat. Sci. **3**(1), 65 (2004).
[39] J. C. Miller, H. H. Pien, D. Sahani, A. G. Sorensen, and J. H. Thrall, J. Natl. Cancer Inst. **97**(3), 172 (2005).
[40] P. R. Moran, Magn., Reson. Imaging **1**, 197 (1982).
[41] P. R. Moran, Annual Meeting, Society of Magnetic Resonance Imaging, San Diego, C.A. (1985).
[42] L. Olah, S. Wecker, and M. Hoehn, J Cereb Blood Metab. **21**, 430 (2001).
[43] W. H. Perman, P. R. Moran, and R. A. Moran, "Effective Data Strategies in Multi Echo NMR Scans… Simultaneous Chem. Shift and Flow" General Electric Medical Systems, System Engineering Technical Report (1985).
[44] E. T. Peterson, I. Zimine, Y-C. L. Ho and X. Golay, Br. J. Radiol. **79**(944), 688 (2006).
[45] T. C. Pilkington, L. T. Bumgardner, and K. D. Strub, "The Use of Pulse NMR Technique for Studying Biological Systems", Proc. 18th Ann. Conf. Eng. In Med. and Biol, Philadelphia, Pensylvania, 28 (1965).
[46] F. Pillekamp, M. Grune, G. Bringr, C. Fanke, U. Uhlenkuken, M. Hoehn, and K-A. Hossmann, Magn. Reson. Imaging **19**, 143 (2001).
[47] J. M. Provenzale, S. Mukundan, and D. P. Barboriak, Radiology **239**, 632 (2006).
[48] J. M. Provenzale, Am. J. Roentgenol. **188**(1), 11 (2007).
[49] D. Salonar, P. R. Moran, and B. M. W. Tsui, Magn. Reson. Imaging **5(S1)**, 37 (1987).
[50] M. Scheidegger, O. Hess, P. Boesiger, "Assessment of Coronary Flow Over the Cardiac Cycle and Diastolic-to-Systolic Flow Ratio with Correction for Vessel Motion" in: Proceedings of the Society of Magnetic Resonance in Medicine, Berkeley, Calf. Society of Magnetic Resonance in Medicine, 498 (1994).
[51] M. Schroeter, C. Franke, G. Stoll, and M. Hoehn, Acta Neuropathologica **101**, 114 (2001).
[52] K. Sebastian, B. S. Markus, M. P. Erik, and P. Boesiger, Magn. Reson. Med. **42**, 970 (1999).

[53] J. R. Singer, and L. E. Crooks, Science **21**, 654 (1983).
[54] C. P. Slichter, *Principles of Magnetic Resonance*, 2nd ed. (reviewed and expanded) (Springer-Verlag, Berlin, Heidelberg, New York, 1978) p.11.
[55] E. Stephan, M. D. Maier, M. B. Scheidegger, K. Liu, E. Schneider, A. Bolinger, and P. Boesiger, J. Magn. Reson. Imag. **5**, 669 (1995).
[56] F. L. Strand, *Physiology: A Regulatory System Approach* (Macmillan Publishing Co. Inc., New York, 1983) p.213.
[57] G. Suryan, "Nuclear Resonance in Flowing Liquid", Proc. Indian Acad. Sci., Section A., 33(2), 107 (1951).
[58] H. Van As, and T. J. Schoafsma, "Non-Invasive Blood Flow Measurement by the NMR - Pulse Method", Soc. of Magn. Reson. In: Med. Book of Abstracts, 1st Annual Meeting, August 16-18, Boston, 182, 147 (1982).
[59] M. T. Viaandingerbroek and J. A. den Boer, *Magnetic Resonance Imaging, Theory and Practice* (Springer-Verlag, Berlin, Heidelberg, New York, 1996).
[60] A. Vieli, U. Moser, S. Maier, D. Meier, and P. Boesiger, Ultrasound in Med and Biol. **15**(2), 113 (1989).
[61] J. Wang, Y. Zhang, R. L. Wolf, A. C. Roc, D. C. Alsop, and J. A. Detre, Radiology **235**(1), 218 (2005).
[62] C. Warmuth, M. Gunther, and C. Zimmer, Radiology **228**, 523 (2003).
[63] M. A. Weber, S. Zoubaa, M. Schlieter, E. Juttler, H. Huttner, K. Geletneky, C. Ittrich, M. P. Lichy, A. Kroll, J. Debus, F. L. Giesel, M. Hartmann, and M. Essig, Neurology **66**(12), 1899 (2006).
[64] V. Wedeen, B. Rosen, D. Chesler, and T. Brady, "MR Velocity Imaging by Phase Display" (Abstract). Program of the third annual meeting of the Society of Magnetic Resonance in Medicine, New York, 742 (1984).
[65] R. E. Wendt, and J. J. Ford, "NMR Pulse Sequence for Rapid Imaging of Flow" (Abstract), Program of the third annual meeting of the Society of Magnetic Resonance in Medicine, New York, 734 (1984).
[66] F. W. Wherli, A. Shimakawa, J. Macfall, and W. Perman, "MR Imaging of Venous and Arterial Flow by a Selective Saturation-Recovery Spin Echo (SSRSE) Method", 3rd Ann Meet. Soc. Mag. Reson. in Med., New York, August 13-17, 744 (1984).
[67] M. Wintermark, M. Sesay, E. Barbier, K. Borbely, W. P. Dillon, J. D. Eastwood, T. C. Glenn, C. B. Grandin, S. Pedraza, J.-F. Soustiel, T. Narai, G. Zaharchuk, J.-M. Caille, V. Dousset, and H. Yonas, Stroke **36(9),** e83 (2005).

Received: 31 May, 2007
Accepted: 20 March, 2008